

Franc Zupanič<sup>1</sup>, Carlos A. Nunes<sup>2</sup>, Gilberto C. Coelho<sup>2</sup>, Paula L. Cury<sup>2</sup>, Gorazd Lojen<sup>1</sup>,

Christian Gspan<sup>3</sup>, Tonica Bončina<sup>1</sup>

<sup>1</sup>Univerza v Mariboru, Fakulteta za strojništvo, Slovenija /

University of Maribor, Faculty of Mechanical Engineering, Slovenia

<sup>2</sup>Univerza v São Paulu, Šola za strojništvo, Brazilija / University of São Paulo, School of Engineering, Brazil

<sup>3</sup>Inštitut za elektromikroskopijo in nanoanalize, Avstrija /

Institut für Elektronenmikroskopie und Nanoanalytik, Austria

# Mikrostruktura kontinuirno ulite nikljeve dentalne zlitine

## Microstructure of a Continuously Cast Ni-based Dental Alloy

### Povzetek

Nikljeve zlitine, ki jih kontinuirno ulijemo, imajo več prednosti v primerjavi s klasično ulitimi zlitinami. Njihova mikrostruktura je bolj drobna, kar zagotavlja boljše mehanske lastnosti, prav tako pa so stroški za kontinuirno litje manjši. V tem delu smo se posvetili predvsem karakterizaciji lite mikrostrukture. Preiskana zlิตina je bila taljena v vakuumski indukcijski peči ter vertikalno kontinuirno lita. Palice premera 10 mm smo raziskali s svetlobnim mikroskopom, vrstičnim in presevnim elektronskim mikroskopom ter energijskodisperzijsko spektroskopijo rentgenskih žarkov. Mikrostruktura je bila sestavljena iz dvofazne osnove (izločki  $\gamma'$  v nikljevi trdni raztopini) ter nizkotaljivega evtektika. Prispevek obravnava tudi procese, ki potekajo med strjevanjem.

**Ključne besede:** kontinuirno litje, nikljeva zlิตina, dentalna zlิตina, mikrostruktura

### Abstract

Ni-based alloys produced by continuous casting possess several advantages when compared to the conventionally cast ones. Their microstructure is much finer, providing better mechanical properties, and the continuous casting process is more cost effective. The main emphasis was given to characterization of the as cast microstructure. The investigated alloy was melted in a vacuum induction furnace and the vertically continuously cast. The rods with the diameter of 10 mm were investigated using light optical microscopy, scanning electron microscopy, transmission electron microscopy and energy dispersive X-ray spectroscopy. The microstructure consisted of the two-phase matrix (Ni-based solid solution and  $\text{Ni}_3(\text{Al},\text{Ti})$ -precipitates), and a low melting eutectic. The contribution also discusses processes taking place during solidification.

**Keywords:** continuous casting, nickel alloy, dental alloy, microstructure.

## 1 Uvod

V današnjem času večino kovinskih polproizvodov izdelujemo s kontinuirnim litjem. Glavne prednosti kontinuirnega litja

## 1 Introduction

Nowadays, the majority of semi-finished metal products are being cast continuously. The main benefits of continuous casting are

so povečanje produktivnosti in kakovosti produktov, kakor tudi zmanjšanje proizvodnih stroškov. Z vakuumskim taljenjem nikljevih zlitin lahko proizvajamo mnoge čistejše zlitine kot z običajnimi izdelovalnimi postopki, kajti takšni ulitki so skoraj brez oksidov in drugih škodljivih vključkov.

Raziskana nikljeva zlิตina se uporablja kot substrat za kovinsko-keramične zobne krone [3]. Glavno prednost v primerjavi z zlatom predstavlja povečan modul elastičnosti in trdnost. Zato so lahko prerezi manjši, zmanjša pa se tudi možnost poškodbe zoba pri pripravi krone. Poleg tega se lahko kovina in keramična krona tesno sprimeta med žganjem, ker je temperaturni razteznostni koeficient nikljevih zlitin podoben temperaturnemu razteznostnemu koeficientu porcelana. Kljub številnim prednostim lahko slabša korozija obstojnost [4] in cena teh zlitin omejita njihovo uporabo.

Pri tej raziskavi smo kontinuirno ulili valjaste palice s premerom 10 mm. Glavni cilj je bil natančno opredeliti lito mikrostrukturo.

## 1 Materiali in metode

Zlิตina je bila kontinuirno ulita na napravi za kontinuirno litje, ki je sestavljena iz vakuumske indukcjske talilne peči Leybold Heraeus in naprave za navpično kontinuirno litje Technica Guss. Sestava zlิตine v masnih odstotkih je bila: 10,10 % Cr, 1,5 % Mo, 5,2 % Si, 0,2 % Ti, 3,5 % Al and 2,1 % Nb. Približno 14 kg zlิตine je bilo taljene v korundnem loncu v vakuumu pri tlaku  $10^{-3}$  do  $10^{-2}$  mbar. Litje je potekalo v varovalni argonski atmosferi. Zlิตina se je strjevala v 10 mm kokili iz bakrove zlิตine. Pri litju je bil uporabljen izmenični vlek, ki je bil sestavljen iz obdobja vlečenja, obdobja mirovanja in obdobja povratnega sunka. Srednja hitrost litja je bila 520 mm/min.

increased productivity and quality of the products, as well as reduced production costs. The vacuum-melting of Ni-based alloys can produce much cleaner alloys in comparison to traditional manufacturing methods because the products are almost free of oxides and other harmful inclusions. In addition, their microstructure is finer, providing better mechanical properties [1,2].

The investigated nickel-based alloy is commonly used as a substructure of metal-ceramic crowns [3]. The main advantage of its usage represents an increased modulus of elasticity and strength as compared with gold. Thus, thinner sections of the alloy can be used, and consequently, tooth destruction during the crown preparation is less probable. Additionally, the metal and ceramic crown can be intimately bonded during firing because the thermal expansion coefficient of Ni-based alloys is well matched to that of the conventional porcelain. Despite many advantages, the corrosion resistance [4] and cost of these alloys somewhat limit their usage.

In the framework of this investigation, cylindrical rods with a diameter of 10 mm were continuously cast, and the main goal of this study was to characterize the as-cast microstructure.

## 1 Materials and Methods

The alloy was continuously cast by using a pilot-scale set up consisting of a Leybold Heraeus vacuum induction melting furnace and a Technica Guss vertical continuous caster. The composition of the alloy (in mass fraction, %) was: 10.10 % Cr, 1.5 % Mo, 5.2 % Si, 0.2 % Ti, 3.5 % Al and 2.1 % Nb. Approximately 14 kg of the alloy was melted under a vacuum of  $10^{-3}$  to  $10^{-2}$  mbar in an alumina crucible. A protective argon

Preiskavo s svetlobnim mikroskopom smo izvedli z mikroskopom Nikon Epiphot 300. Uporabili smo tudi vrstična elektronska mikroskopa FEI SIRION NC in FEI Quanta 3D ter presevni elektronski mikroskop FEI Tecnai F20. Vzorec za presevno elektronsko mikroskopijo je bil odvzet na določenem mestu z napravo fokusirani ionski curek (FEI Nova 200).

## 2 Rezultati in diskusija

Površina palice z ustnikovim znamenjem (primary witness mark) in znamenjem združitve (secondary witness mark) ter makrostruktura palice sta bili podobni kot v prejšnjih delih [2]. Makrostruktura je bila v glavnem sestavljena iz steberastih kristalov, ki so segali od površine do središča palice. Kristalna zrna so rastla z značilno dendritno morfologijo (sl. 1). Razdalja med primarnimi in sekundarnimi vejami se je povečevala s povečevanjem razdalje od površine palice. Občasno se je v središču palice pojavila nitasta poroznost.

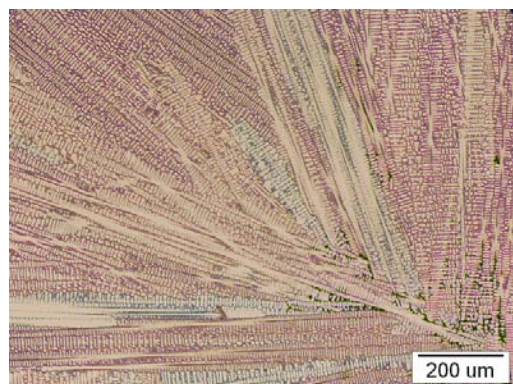
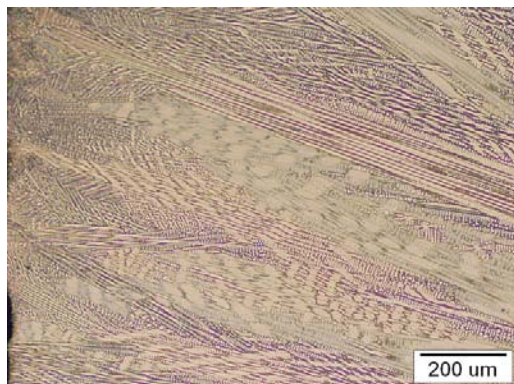
V vzdolžni smeri je makrostruktura periodična, kar izvira iz izmeničnega načina

atmosphere was used during continuous casting. The alloy solidified within a water-cooled copper-alloy mould ( $\varnothing$  10 mm). The rod was extracted out of the mould using an “alternating drawing mode” consisting of the drawing stroke, the resting period and the reverse stroke, and the average casting speed was 520 mm/min.

Light microscopy (LM) work was done using Nikon Epiphot 300. The scanning electron microscopy (SEM) was carried out in a FEI SIRION NC and FEI Quanta 3D, and the transmission electron microscopy (TEM) in a FEI Tecnai F20. The TEM specimen was cut out at a specific site using a focussed ion beam (FIB) in a FEI Nova 200.

## 2 Results and Discussion

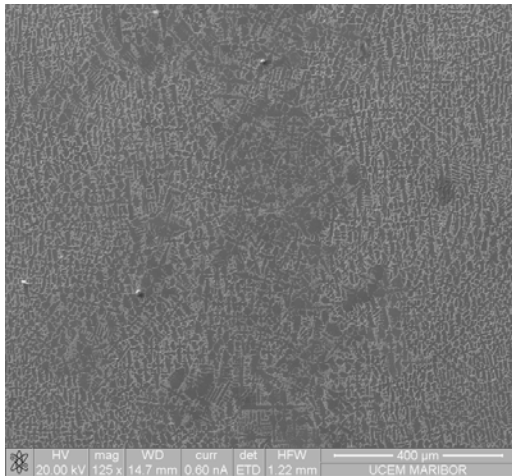
The surface of the rod with primary and secondary witness marks, as well as the macrostructure, was very similar to those reported in a previous work on continuous casting [2]. The macrostructure mainly consisted of columnar grains, extended from the rod surface towards the rod's centre.



**Slika 1:** Svetlobna mikroposnetka prečnega prereza a) roba in b) središča palice.

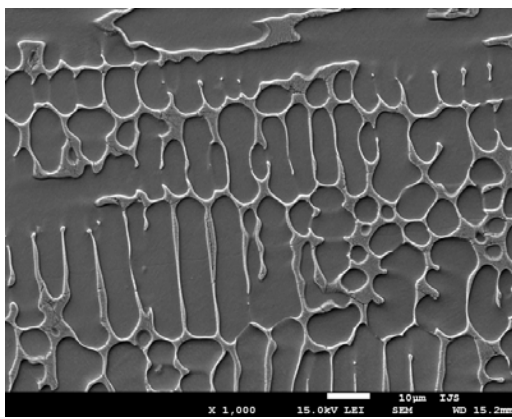
**Figure 1:** Light-optical micrographs a) at the edge, b) at the centre of the rod (transversal cross-section)

vlečenja [1]. Valovna dolžina periodičnega vzorca je bila zelo blizu dolžini cikla. Ozko območje ob površini je bilo sestavljeno iz naključno orientiranih kristalnih zrn.



**Slika 2:** Elektronski mikroposnetek z odbitimi elektroni prikazuje vzdolžni prerez središča palice

**Figure 2:** A backscattered electron micrograph at a centre of the rod (longitudinal cross-section)



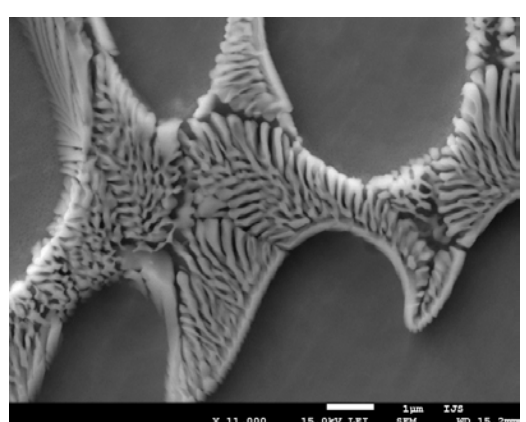
**Slika 3:** Mikroposnetka z odbitimi elektroni v središču palice (vzdolžni prerez): a) pregledna slika, b) povečana slika meddendritnega prostora z binarnim evtektikom

**Figure 3:** Backscattered electron micrograph at a centre of the rod (longitudinal cross-section): a) an overview image, b) magnified image of the interdendritic spaces, with the binary eutectic

The grains grew with a typical dendritic morphology (Figure 1). The distances between the primary and secondary arms increased with increasing distance from the rod surface. Occasionally, solidification porosity was present at the rod's centre.

In the longitudinal direction, the rods clearly showed periodic macrostructure caused by the alternating drawing mode similar as in [1]. The wavelength of the periodic pattern corresponded closely to the cycle length. A shallow chill zone composed of randomly oriented crystal grains was present at the rod surface. Otherwise, columnar grains prevailed. They extended from the chill zone to the rod centre, except for some places (Figure 2). The  $\gamma$ -grains propagated almost perpendicular to the rod surface during drawing stroke, while they grew inclined to the casting direction during the resting period.

Figure 3 shows a typical microstructure. It consisted of  $\gamma$ -dendrites and binary eutectic ( $\gamma + \text{Nb}_6\text{Ni}_{16}\text{Si}_7$ ). The intermetallic eutectic phase  $\text{Nb}_6\text{Ni}_{16}\text{Si}_7$  has a morphology typical for a complex regular eutectic.



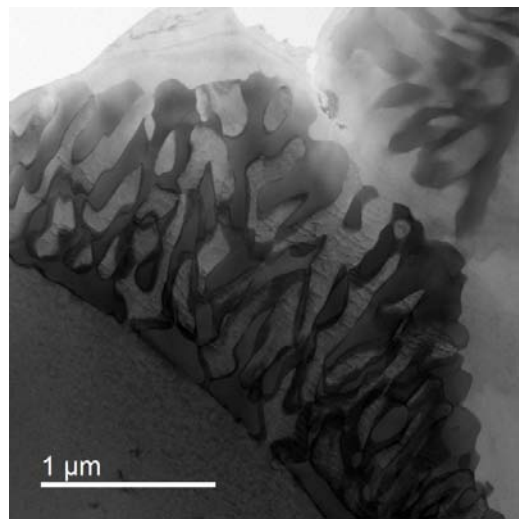
V večjem delu prereza so prevladovala usmerjena kristalna zrna. Razen na nekaterih mestih so se vselej raztezala od hitroohlajenega območja ob površini pa vse do središča palice (Sl. 2). Zrna  $\gamma$  (to je oznaka za trdno raztopino na osnovi niklja), ki so nastala med vlekom, so bili praktično pravokotna na površino kokile, medtem ko so zrna med obdobjem mirovanja rastla v smeri litja.

Slika 3 prikazuje značilnomikrostrukturo. Sestavljena je iz  $\gamma$ -dendritov in binarnega evtektika ( $\gamma + \text{Nb}_6\text{Ni}_{16}\text{Si}_7$ ). Intermetalna evtektična faza  $\text{Nb}_6\text{Ni}_{16}\text{Si}_7$  ima obliko, ki je podobna kompleksno urejenemu evtektiku. Natančnejša raziskava s presevnim elektronskim mikroskopom je pokazala, da  $\text{Nb}_6\text{Ni}_{16}\text{Si}_7$  nastane na dendritnih vejah in potem raste v preostalo talino (sl. 4a). Ta faza se lahko hitro razveja, tako da se z lahkoto prilagaja spremembam strjevalnih parametrov ter razpoložljivemu prostoru v meddendritnem območju. Značilne velikosti

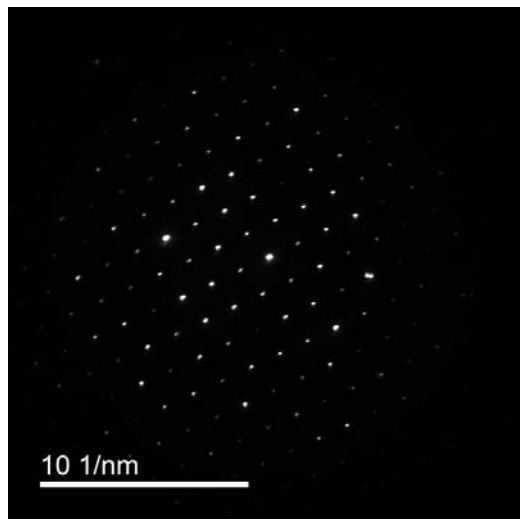
Close examination using TEM showed that  $\text{Nb}_6\text{Ni}_{16}\text{Si}_7$  formed on dendritic arms of  $\gamma$ , and then grew into the remaining liquid (Fig. 4a). This phase can branch rapidly, thus easily responding to variation in solidification conditions, and adapting to the available space in the interdendritic region. Typical sizes of the eutectic cells were few micrometres, while the distances between lamellas were few tenths of micrometre.

Fig. 4b shows the selected area diffraction pattern (SADP) taken along a [011] axis of FCC-  $\text{Nb}_6\text{Ni}_{16}\text{Si}_7$ . From the positions of diffraction spots, it was calculated that the lattice spacing of  $\text{Nb}_6\text{Ni}_{16}\text{Si}_7$  was  $1.129 \text{ nm} \pm 0.010 \text{ nm}$ .

Fig. 5 shows that the matrix was not only of Ni-solid solution  $\gamma$ , but also possessed precipitates  $\gamma'-\text{Ni}_3(\text{Al},\text{Ti})$ . Even more, the volume fraction of the precipitates was much larger than the volume fraction of the  $\gamma$ -phase. SADP shows that  $\gamma$  and  $\gamma'$  have almost the same lattice parameters,



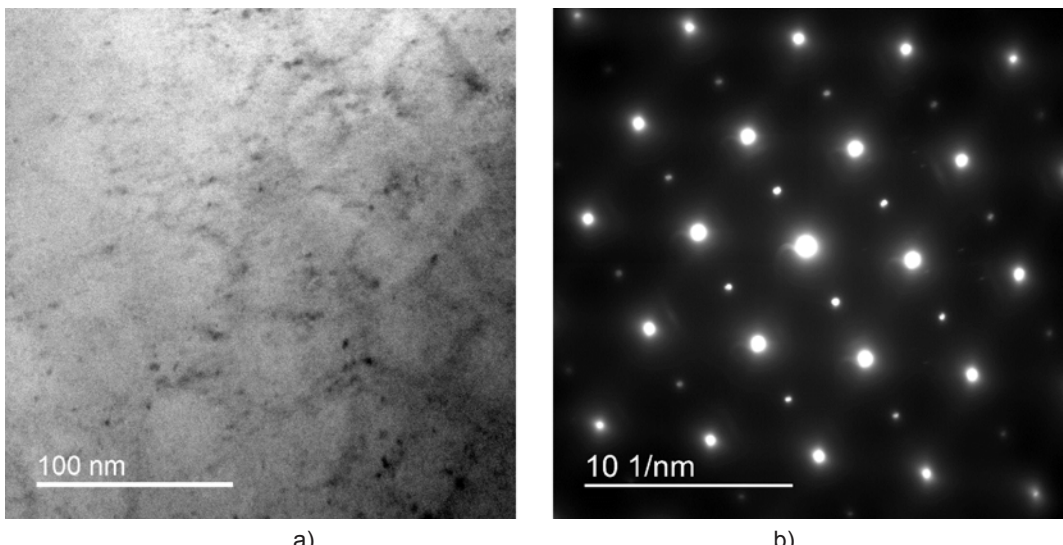
a)



b)

**Slika 4:** Presevna elektronska mikroskopija: a) meddendritni prostor z binarnim evtektikom, b) ukloški vzorec izbranega območja (SADP) faze  $\text{Nb}_6\text{Ni}_{16}\text{Si}_7$ , s consko osjo vzporedni smeri [011]

**Figure 4:** Transmission electron microscopy: a) interdendritic space with the binary eutectic, and b) the selected area diffraction pattern taken along [011] axis of the eutectic phase:  $\text{Nb}_6\text{Ni}_{16}\text{Si}_7$



**Slika 5:** Presevna elektronska mikroskopija: a) osnova ( $\gamma + \gamma'$ ), in b) in njen uklonski vzorec (SADP)

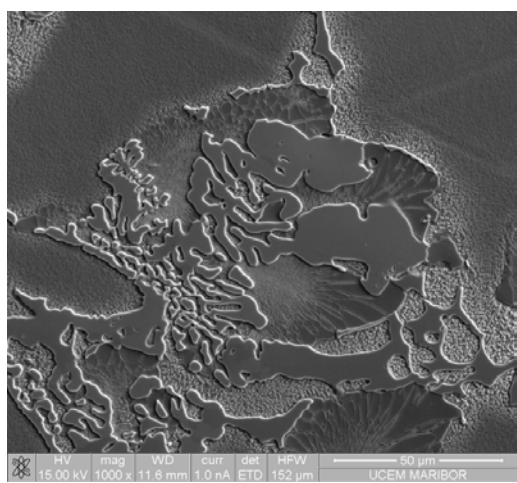
**Figure 5:** Transmission electron microscopy: a) the matrix ( $\gamma + \gamma'$ ), and b) its selected area diffraction pattern (SADP).

evtektičnih celic so nekaj mikrometrov, medtem ko so bile razdalje med evtektičnimi lamelami nekaj desetink mikrometra.

Slika 4b prikazuje uklonski vzorec izbranega območja (SADP), pri čemer je bila conska os ploskovno centrirane kubične faze  $Nb_6Ni_{16}Si_7$  vzporedna s smerjo [011]. Iz položaj uklonskih lis smo izračunali, da je bila mrežna konstanta faze  $Nb_6Ni_{16}Si_7$  enaka  $1.129\text{ nm} \pm 0.010\text{ nm}$ .

Slika 5 kaže, da v osnovi ni bila samo faza  $\gamma$ , temveč tudi izločki  $\gamma'-Ni_3(Al,Ti)$ . Še več, prostorninski delež teh izločkov je presegal prostorninski delež faze  $\gamma$ . Uklonski vzorec izbranega območja (SADP) je pokazal, da sta imela  $\gamma$  in  $\gamma'$  skoraj enak mrežni parameter. Njegova vrednost je znašala  $a = 0.328\text{ nm} \pm 0.003\text{ nm}$ . Izločki  $\gamma'$  so nastali med ohlajanjem v trdnem stanju, pod temperaturo solvus te zlitine.

Slika 6 prikazuje mikrostrukturo precizijsko ulitega vzorca. Razvidno je, da so mikrostrukturne sestavina dosti bolj



**Slika 6:** Mikroposnetek z odbitimi elektroni precizijsko ulite Ni-zlitine

**Figure 6:** Backscattered electron micrograph of the investment cast Ni-alloy

grobe. Strjevanje pri precizijskem litju je namreč počasnejše, zato nastanejo bolj grobe intermetalne faze. Navzočnost bolj grobih faz lahko podaljša čase taljenja v zobnem laboratoriju. Še več, makroizceje so v palicah, ulitih s precizijskim litjem, bolj pogoste in tudi izrazite, zato imajo lahko končni produkti neenake kemične sestave in s tem tudi različne tehnološke lastnosti.

Glede na vse rezultate lahko rečemo, da dobimo pri kontinuirnem litju mikrostrukturo, ki so bolj primerni za zobotehniške aplikacije, kot tiste, ki nastanejo pri precizijskem litju.

### 3 Zaključki

V tem delu smo raziskali mikrostrukturo kontinuirno ulitih palic iz nikljeve zlitine, ki se uporablja za zobotehniške aplikacije. Mikrostruktura je bila pretežno sestavljena iz dendritne osnove, v kateri sta bili faza  $\gamma$  in izločki  $\gamma'$ . V meddendritnih prostorih je bil binarni evtektik ( $\gamma + \text{Nb}_6\text{Ni}_{16}\text{Si}_7$ ). Izločki  $\gamma'$  so nastali med ohlajanje pri izločanju iz trdne raztopine pod temperaturo solvus.

Mikrostruktura, ki je nastala pri kontinuirnem litju, je bila drobnejša kot v precizijskih ulitkih. Poleg tega je imela manj makroizceje ter je bila precej čistejša. Na tej osnovi lahko upravičeno pričakujemo, da bo v naslednjih letih večina Ni-zlitin za zobotehniko izdelanih s kontinuirnim litjem.

### 4 Acknowledgements

To delo je podprla agencija ARRS v okviru bilateralnega projekta med Slovenijo in Brazilijo, št. BI-BR/12-14-003. Del dela je bil tudi podprt s strani Evropske skupnosti. TEM-raziskave na TU Graz so prejele finančno pomoč s strani 7. okvirnega programa: Grant Agreement 312483

and are coherent than in other nickel-based superalloys. The evaluated lattice parameters of both phases were:  $a = 0.328 \text{ nm} \pm 0.003 \text{ nm}$ . The  $\gamma'$ -precipitates formed during cooling in the solid state, below the alloy's solvus temperature.

Fig. 6 shows the microstructure of the investment cast sample. It is evident that the microstructural constituents are much coarser. The solidification of the investment cast rods was rather slow, resulting in formation of coarse intermetallic phases. The presence of coarse phases can increase the melting time in dental laboratory. In addition, macrosegregations are rather frequent in investment cast rods, thus the final parts can possess different chemical compositions, and thus different technological properties.

Therefore, continuous casting can produce microstructures that are more convenient for dental applications than those formed by investment casting.

### 3 Conclusions

In this work, the microstructure of continuously cast rods of a Ni-based alloy for dental applications was investigated. The microstructure composed mainly of the dendritic columnar matrix:  $\gamma$ -solid solution and  $\gamma'$ -precipitates. In the interdendritic regions, a binary eutectic formed ( $\gamma + \text{Nb}_6\text{Ni}_{16}\text{Si}_7$ ).  $\gamma'$ -precipitates formed during cooling below the alloy's solvus temperature.

The microstructure formed during continuous casting was much finer than that formed during investment casting. In addition, the alloy possessed much less macrosegregation and it was much cleaner. Thus, it is expected that in the following years, most of the Ni-based dental alloys will be continuously cast.

- ESTEEM2 (Integrated Infrastructure Initiative–I3).

#### 4 Acknowledgements

This work was supported by the ARRS under the framework of the Slovenian-Brazilian bilateral project BI-BR/12-14-003. Part of the work was carried out with the support of the European Community. The TEM investigations in TU Graz have received funding from the European Union Seventh Framework Programme under Grant Agreement 312483 - ESTEEM2 (Integrated Infrastructure Initiative–I3).

#### Viri / References

1. E. Herrmann, D. Hoffman (ed): "Handbook on Continuous Casting", V-VI; Aluminium-Verlag, Düsseldorf, 1980
2. Zupanic, F., T. Boncina et al., "Microstructural evolution on continuous casting of nickel based superalloy Inconel® 713C." Materials Science and Technology, **18**(2002)7, 811-819.
3. J. C. Wataha, Alloys for prosthetic restorations, The Journal Of Prosthetic Dentistry, 87 (2002), 351-363
4. M.J. Perricone and J.N. Dupont, Effect of Composition on the Solidification Behavior of Several Ni-Cr-Mo and Fe-Ni-Cr-Mo Alloys, Metallurgical And Materials Transactions A, 37A, (2006), 1267-1280